Transactions on Engineering and Computing Sciences - Vol. 11, No. 4
Publication Date: August 25, 2023
DOI:10.14738/tecs.114.15079.
Kim, Y. M. (2023). ADDENDUM TO 'A Study on the Eigenmodes Constructed in the Conductor Backed Coplanar Waveguide'. Transactions on Engineering and Computing Sciences, 11(4). 21-33.



ADDENDUM TO 'A Study on the Eigenmodes Constructed in the Conductor Backed Coplanar Waveguide'

Yeong Min Kim
Kyonggi University, Korea

ABSTRACT

In this study, finite element method has been carried out to calculate the eigenmode formed in the micro-script, conductor-backed slot line and conductor-backed coplanar waveguides. The eigenmodes have been represented with the electric field, 3D electric potential and electric equipotential contours. The electric potentials together with electric fields have improved understanding of eigenmodes of the waveguides. In particular, the electric potentials have been useful for revealing multiple and complex mixed peaks. In previous manuscript, the eigenmodes of the spectra have been mainly analyzed using electric fields. Comparing these results, it could be said that the interpretation based on the potential difference along with the electric field is more reliable. In other words, if the computational capacity of the personal computer is large enough to calculate the electric field and potential simultaneously, calculating these factors and analyzing the spectra based on them would result in a more reliable interpretation.

Keywords: eigenmode, finite element method, electric field, electric potential, electric equipotential contour, micro-script waveguide, conductor-backed slot line waveguide, conductor-backed coplanar waveguide.

INTRODUCTION

Previously, the study for CBCPW (Conductor-Backed Coplanar Waveguide) etc. have been carried out using FEM (Finite Element Method) [1]. In this paper, it has been tried to improve the understanding of the eigenmodes and clarify their physical properties through the representation of electric fields. The eigenpairs have been consist with the vector electric field and the scalar electric equipotential. Those eigenpairs have been the column matrix of the similarity transform matrix. This matrix has been the result of a Krylov-Schur iterative method for FEM. This iteration method compresses large matrices into smaller one and adopts only a few significant components. What this study pays attention to has been the similarity transform matrix leading the iterative method. The column matrix has contained the eigenmodes that describe electric fields and potentials. The diagonal components of Schur matrix resulted from the iterative process have been compared to the previous one. When the deviation converged to a predetermined value, the similarity transform matrix that led to this process has been selected as an eigenmode. A column matrix has a dimension equal to the number of edges plus the number of nodes. The components of the edge vectors have been grouped into corresponding triangular elements. The eigenmodes of the electric field have been plotted in vector form at the barycentric point of the triangular element by combining them. The components of the node points have been grouped into corresponding triangular elements. The

eigenmodes of the electric potential have been plotted into the 3D potential and the electric equipotential contours. Equipotential lines have been drawn by connecting the points obtained from interpolating the potential values of nodal points of the triangular element. In previous manuscripts, the electric field eigenmodes were intensively applied when revealing the characteristics of waveguides. Including the electric equipotential makes the matrices to be processed in the FEM calculations becoming larger. There has been a limit to revealing the characteristics of a waveguide using only the electric field eigenmode. Several electric equipotential and 3D representations have been used as auxiliary when discussing physical properties driven by electric field eigenmodes. For a more accurate and high-quality analysis, it would be better to combine the potential eigenmode with that of the electric field.

In this study, we discuss the physical properties of waveguides by combining eigenmodes of the electric field, 3D electric potential and that of the equipotential contours. These eigenmodes are complementary to each other. If the resolution of spectra is reduced due to the mixing of several equipotential lines, the electric field eigenmodes can compensate it and vice versa. As a result, it would be possible to improve the understanding of the characteristics of the waveguide, which had not been discussed in previous studies, with the aid of equipotential lines. The eigenmodes to be found by applying the electric field, 3D potential and equipotential are MSW (Microscript Waveguide), CBSLW (Conductor-Backed Slot Line Waveguide) and CBW (Conductor-Backed Coplanar Waveguides).

In 1962 C. P. Wen firstly demonstrated a CPW (Coplanar Waveguide) fabricated on a dielectric substrate [2]. Since that time, tremendous progress has been made in CPW based MICs (Microwave integrated circuits) as well as MMICs (Monolithic Microwave Integrated Circuits). The waveguide mentioned above is a typical CPW variant with a ground plane on the entire back side of the board. These waveguides exhibit unique characteristics along with CPW and are applied to various application fields. Therefore, it would be a meaningful task to reveal the characteristics of the eigenmodes they form in these waveguides [3][4].

THE WAVEGUIDES

The waveguides covered in this study are the same as in previous studies. Those are MSW, CBSLW, and CBCPW and represent the structures shown in the following figures.

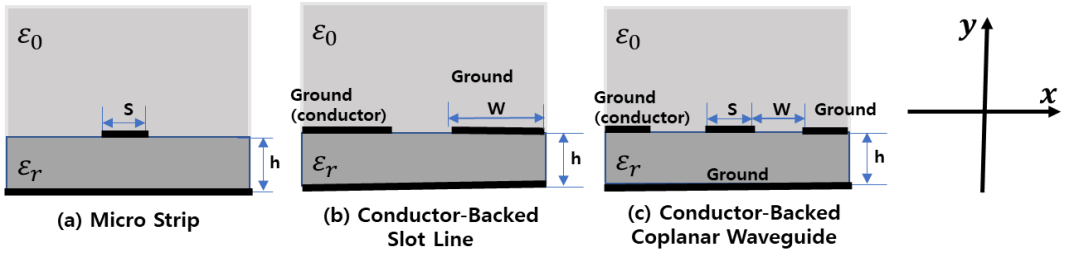


Figure 1. Waveguides

Among the waveguides, what is different from the previous ones is that coplanar waveguide is replaced with CBSLW. The reason is that the resolution of the CBSLW spectrum is better than that of the CPW. All waveguides have the rectangular cross section of the same width, height

and area. The height and width of the waveguide must be sufficient size for building the eigenmodes of the electromagnetic waves in it. Especially, the area of the waveguide is an important factor in determining the characteristics of the eigenmodes. This area must be sufficiently large to be considered that the wave emitted by the signal conducting track is disappeared from its edge. This is because it can cause unwanted higher order modes to propagate in the waveguide. The upper part of the dielectric is considered free space and the permittivity is assumed to be $\varepsilon_o = 1$. FEM perform the calculation including this area in order to know how the electromagnetic waves emitted by the signal conduction track spread out into free space. The relative permittivity of the dielectric substrate has larger value $\varepsilon_0 < \varepsilon_r$ than the free space. According to Snell's law, electromagnetic waves are expected to be concentrated in areas with a larger permittivity. The height of the dielectric substrate is 1/4 of its width. The ground conductor and signal conducting track onto the substrate are symmetrically arranged with respect to the vertical center line of waveguides. The width of the signal conducting track is 1/5 of that of substrate. In CBCPW, this distance has a profound effect on determining the nature of the eigenmode. It has been known that as this distance increases, the eigenmode takes on a shape similar to MSW. In other words, as this distance increases, the influence of the ground conductors has less effect on the electromagnetic waves emitted from the signal conducting track. To facilitate the computation of the FEM, the cross section of the space of waveguide is decomposed into a mesh of triangular elements.

The most important things in FEM calculations are the edges and nodes of these triangular elements. Edges are defined as vectors because they are used to compute the electric field. As mentioned in the previous manuscript, the common edges of neighboring triangular elements must point in the same direction. In this way, a continuous and consistent electric field distribution can be implemented. The relation of the edge direction of the mesh elements is represented in the figure 2(a). The nodes of triangular elements are components for calculating the electric 3D potential and equipotential contours. They are described as scalar quantities. As shown in the figure 2(b), equipotential lines are drawn by connecting the points obtained from interpolating the potential values of nodal points of the triangular element. The equipotential lines are formed by dividing the difference between the maximum and minimum potential values represented by nodes with 20. As shown in this figure, the length and the orientation of one edge is shared by two triangular elements, and a node is shared by six triangular elements.

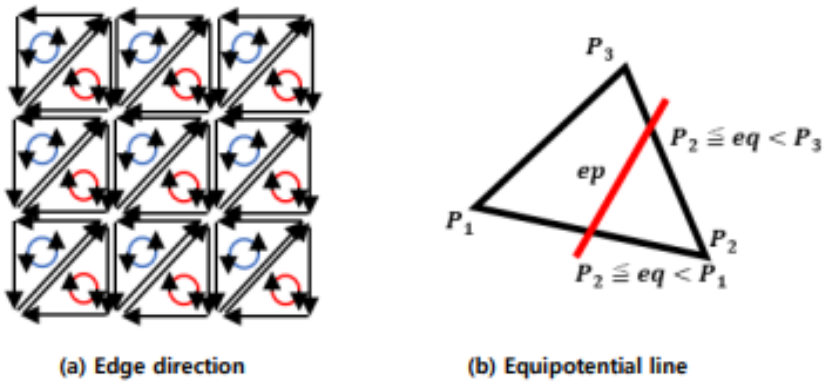


Figure 2. Schematic representation of mesh

FEM THEORY

Generally, it is well known that the above-mentioned waveguides form quasi-TEM modes. Those waveguides include some TE and TM modes independently but the TEM eigenmodes are dominant comparing to them. This is because the conductors are partially attached to the surface of the substrates. The conducting surface is very important in determining the eigenmode. The Neumann and Dirichlet boundary condition are applied for TM and

TE modes respectively. For the perfect conductor attached on the dielectric substrate, the electric field only incident on it perpendicularly. Tangential components of the electric field are not allowed along the conductor in the equilibrium state. To apply this fact to FEM, the edge vectors and nodes of the triangular elements each contacting the conductor boundary are excluded for TE mode. In FEM process, those components describe the electric field and electric potential respectively. The boundary conditions mentioned above cannot be applied to the rest of the waveguide where conductors are excluded. TM mode predominates in this area where conducting material is excluded. In a structure in which TE and TM characteristics are mixed, those modes are combined into quasi-TEM modes. In this manuscript, quasi-TEM eigen properties are considered for above mentioned waveguides. The theory base on the vector Helmholtz equation. FEM is applied to construct matrix eigen equations that are solvable through numerical analysis [5]. In FEM calculating process, TM is similarly described to that of TE. These modes can be consistently described together by the function $\vec{F}$. For convenience of discussion, it is assumed that the cross section and the axis of the waveguides are the xy-plane and z-axis of the Cartesian coordinate, respectively. In this coordinate, the vector Helmholtz equation is given by

$$\vec{\nabla} \times \left(\bar{\bar{p}}\vec{\nabla} \times \vec{F}\right) - k_0^2 \bar{\bar{q}}\vec{F} = 0 \tag{1}$$

and the wavefunction

$$\vec{F} = \left(F_x\hat{x} + F_y\hat{y} + F_z\hat{z}\right)^{e-j\beta z} \tag{2}$$

Where β is the propagation constant and for electric field strength $\vec{F} = \vec{E}$, $\bar{\bar{p}} = \frac{1}{\mu_r}$ (μ_r: relative permeability μ/μ_o) $\bar{\bar{q}} = \bar{\bar{\varepsilon}}_r$ (ε_r: relative permitivity $\varepsilon/\varepsilon_o$), and for magne-tic field strength $\vec{F} = \vec{H}$ (Magnetic field strength), $\bar{\bar{p}} = \frac{1}{\bar{\bar{\varepsilon}}_r}$, $\bar{\bar{q}} = \bar{\bar{\mu}}_r$. In this study, it is assumed that the waveguides have the homogeneous dielectric substrates. So, the following relation is reflected in the tensor matrix of the equation

$$\begin{cases} \varepsilon_{ij} = \varepsilon, \mu_{ij} = \mu \; when \; i = j \\ \varepsilon_{ij} = 0, \mu_{ij} = 0 \; when \; i \neq j \end{cases} \tag{3}$$

For the convenience of the description, the following calculating process focus on the electric field. By separating the transverse vector fields and the z-components scalar potential, equation (1) for electric field can be described as

$$\vec{\nabla}_t \times \left(\vec{\nabla}_t \times \vec{E}_t\right) + \frac{1}{\mu_r}\left(\beta^2 \vec{\nabla}_t E_z + \beta^2 \vec{E}_t\right) = k_0^2 \varepsilon_r \vec{E}_t \tag{4}$$

$$-\frac{1}{\mu_r}\left[\vec{\nabla}_t \cdot \left(\vec{\nabla}_t E_z + \beta \vec{E}_t\right)\right] = k_0^2 \varepsilon_r E_z \tag{5}$$

where

$$\vec{E}_t = E_x \hat{x} + E_y \hat{y} \tag{6}$$

When the vector Helmholtz equation is divided into two equations, one equation is described by the tangential edge vectors and other by the node components of the triangular element. Then the transverse electric field is approximately given by the tangential edge vectors of a triangular element as follows

$$\vec{E}_t = \sum_{m=1}^{3} e_{tm} \vec{W}_{tm} \tag{7}$$

where $\vec{W}_{tm}$ is the edge m vector of the triangular element. Its components are given by the simplex coordinate as like

$$\vec{W}_{t1} = L_{t1}\left(a_3 \vec{\nabla}_t a_2 - a_2 \vec{\nabla}_t a_3\right) \tag{8}$$

$$\vec{W}_{t2} = L_{t2}\left(a_1 \vec{\nabla}_t a_3 - a_3 \vec{\nabla}_t a_1\right) \tag{9}$$

$$\vec{W}_{t3} = L_{t3}\left(a_2 \vec{\nabla}_t a_1 - a_1 \vec{\nabla}_t a_2\right) \tag{10}$$

WhereL_{ti} is a length of the edge connecting the nodal points j and k. The scalar potential of z-component equation is described by the nodal based first order Lagrangian interpolation functions as

$$E_z = \sum_{i=1}^{3} e_{zi} a_i \tag{11}$$

wherea_i is the simplex coordinate of node i. The simplex coordinates are given with nodal points of the triangular element of Figure 3.

$$\begin{pmatrix} a_1 \\ a_2 \\ a_3 \end{pmatrix} = \begin{bmatrix} 1 & 1 & 1 \\ x_1 & x_2 & x_3 \\ y_1 & y_2 & y_3 \end{bmatrix}^{-1} \begin{pmatrix} 1 \\ x \\ y \end{pmatrix} \tag{12}$$

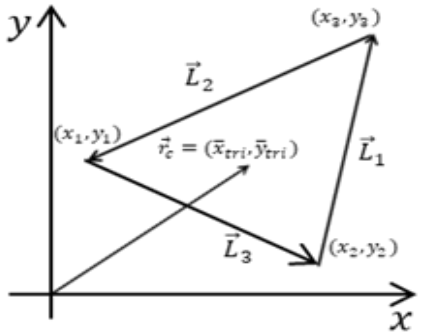


Figure 3. The simplex coordinate.

From figure 3, the relationship between tangential edge vectors and nodes of a triangular element can be identified.

The vector Helmholtz equation for the triangular element can be made into the matrix eigen equation

$$\begin{bmatrix} S_{el(tt)} & S_{el(tz)} \\ S_{el(zt)} & S_{el(zz)} \end{bmatrix} \begin{pmatrix} e_t \\ e_z \end{pmatrix} = \begin{bmatrix} T_{el(tt)} & 0 \\ 0 & T_{el(zz)} \end{bmatrix} \begin{pmatrix} e_t \\ e_z \end{pmatrix} \tag{13}$$

where each component of the square matric are given as

$$S_{el(tt)} = \frac{1}{\mu_r} \iint_{\nabla} \left(\vec{\nabla}_t \times \vec{W}_{tm}\right) \cdot \left(\vec{\nabla}_t \times \vec{W}_{tn}\right) ds - \frac{\beta^2}{\mu_r} \iint_{\nabla} \left(\vec{W}_{tm} \cdot \vec{W}_{tn}\right) ds \tag{14}$$

$$S_{el(tz)} = \frac{\beta^2}{\mu_r} \iint_{\nabla} \left(\vec{W}_{tm} \cdot \vec{\nabla}_t a_j\right) ds \tag{15}$$

$$S_{el(zt)} = \frac{\beta^2}{\mu_r} \iint_{\nabla} \left(\vec{\nabla}_t a_j \cdot \vec{W}_{tm}\right) ds \tag{16}$$

$$S_{el(zz)} = \frac{\beta^2}{\mu_r} \iint_{\nabla} \left(\vec{\nabla} a_i \cdot \vec{\nabla} a_j\right) ds \tag{17}$$

$$T_{el(tt)} = \varepsilon_r \iint_{\nabla} \left(\vec{W}_{tm} \cdot \vec{W}_{tn}\right) ds \tag{18}$$

$$T_{el(zz)} = \varepsilon_r \beta^2 \iint_{\nabla} a_i \cdot a_j ds \tag{19}$$

The global eigen equation is resulted by combining these element matrices for total meshes.

$$[S]\{e_{tot}\} = k_0^2 [T]\{e_{glob}\} \tag{20}$$

As results, the eigenmodes are obtained by similarity transforming the matrix eigen equation into the Schur matrix. The column vectors of the similarity transforming matrix are the eigenmodes and the diagonal components of the Schur matrix are eigenvalues.

In general, the dimensionality of the matrix eigen equation is very large. The personal computer cannot perform the calculation especially for the inverse matrix of large dimensionality in ordinary manner. Therefore, a sophisticated method such as the Krylov-Schur iteration method is applied to overcome this problem [6][7]. It is well known that this method gives several prominent eigenmodes for the waveguides robustly. Previously, this iteration method has applied to the varied optical fiber and revealed their eigen properties of propagating waves.

To apply this iteration method, the global eigen equation is firstly converted to the shift invert form as like

$$\frac{1}{k_0^2-\sigma}\{e_{glob}\} = \frac{T}{[S]-\sigma[T]}\{e_{glob}\} = [M]\{e_{glob}\} \tag{21}$$

The Krylov-Schur iteration method is applied to the matrix $[M]$. By doing so, this strategy may be more efficiently implemented in finding specific eigenmodes at σ value.

RESULT AND DISCUSSION

Previously, FEM (Finite Element Method) has been carried out to investigate the properties of the eigen pairs of the micro waveguides. The eigen pair consists of the transverse electric field and potential created in the waveguide. Those are obtained simultaneously as a result of the Krylov-Schur iteration process. This iterative method compresses the large matrix into smaller one to calculate effectively the inverse matrix. After several iterations, if the result of the eigen pairs shows a small deviation compared to the previous one, the column components of the similarity transform matrix are accepted as the eigen pairs. What was obtained is a few elements in this process, but they represent the prominent characteristics of the eigen pairs. The electric field and potential obtained in this way complement each other and accurately describe the eigen properties of the waveguides. But in the previous manuscript, the electric field was dominantly emphasized in describing the properties of the waveguide, and the electric potential played an auxiliary role to the electric field. For improving interpretation of eigen properties, it is effective to use electric potentials along with electric fields. If it is difficult to interpret the eigen property as an electric field, compensating it with electric potential improves understanding and vice versa. The electric field is expressed as a vector value at the barycentric point by combining the edge vectors of the triangular elements. The edge vector of the triangular element in the mesh was described in the previous manuscript. In this study, the eigen potentials are shown with electric a three-dimensional representation and an electric equipotential. Equipotential lines are drawn by connecting the points obtained from interpolating the potential values of nodal points of the triangular element. In order to improve the resolution of the spectral line, the electric potential is also shown as a 3D image. The use of 3D images along with equipotential lines enable more improved interpretation for spectral lines. In other word it is possible to use 3D images along with equipotential lines enable correct

interpretation for spectral lines. The schematic representation of figure 4 shows the spectra of micro-script. This figure consists of the eigen electric field, 3D electric potential, and electric

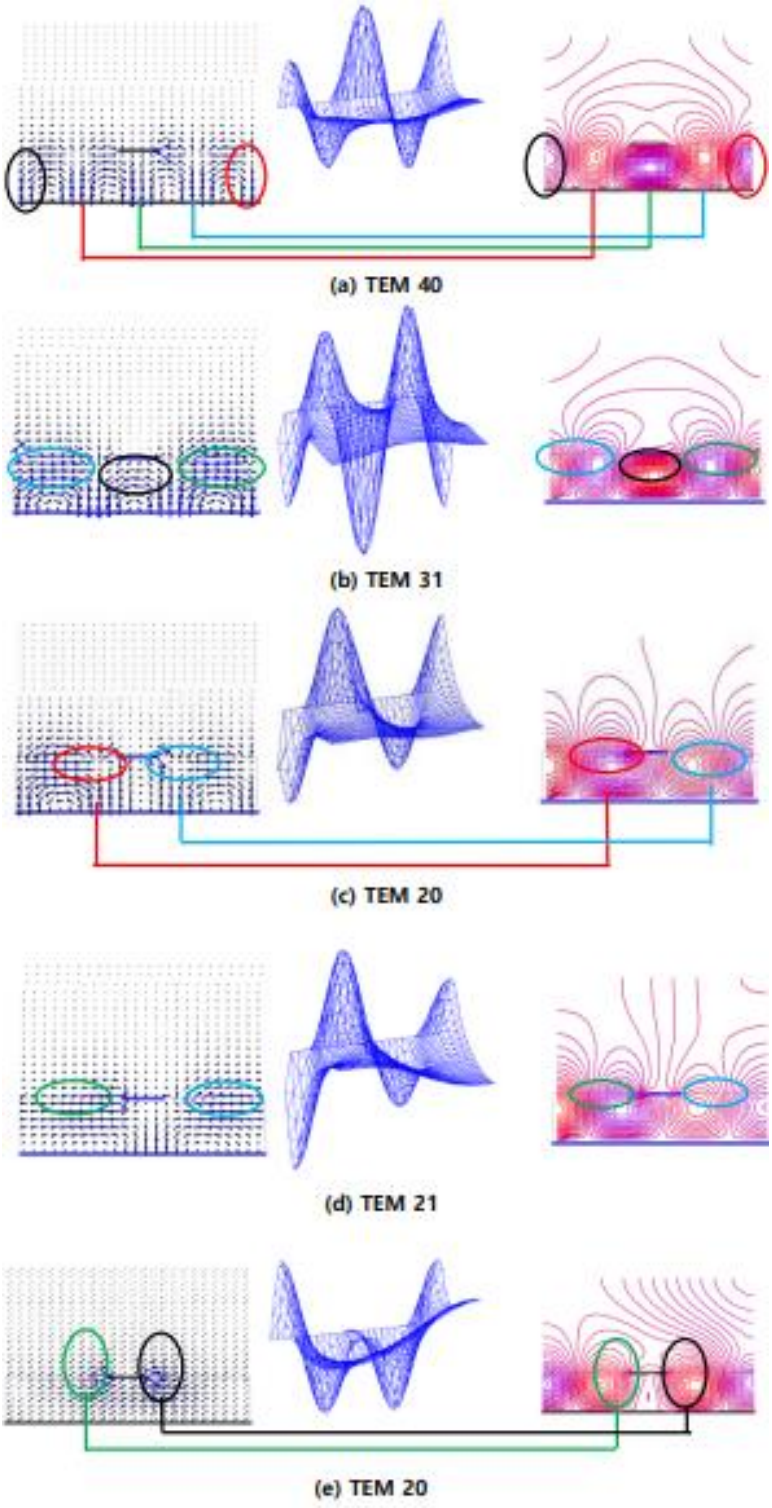


Figure 4. Spectra of the Micro-script Waveguide

equipotential projected into the plane of z-direction. In these spectra, the contour line of electric equipotential and the direction of electric field can be clearly identified. However, determining eigenmodes based on superficial spectra alone can be misleading. To determine clearly the eigenmodes the spectra of electric field and electric equipotential are compared with each other. Since space gradient of the potential is the electric field, positions of the extreme electric potential correspond to regions where the electric field strength is strong. Figure 4(a) shows lines and circles connecting between the position of extreme equipotential and its corresponding electric field pairs. Each color-coded line indicates the equipotential lines and their corresponding electric fields. In particular, the components inside the circles marked on the left and right sides of the waveguide clearly show the corresponding relationship between the electric field and the equipotential line. That is, the greater the strength of the electric field, the more clearly the corresponding extreme equipotential lines appear. Therefore, it can be said that the spectral line of figure 4(a) describes the eigenmode TEM 40. Together with 3D dimensional images, such eigenmode determination is more reliable. As can be seen from the 3D image, there are three peaks inside the waveguide and half-peaks on the left and right sides of it, so total four peaks. From these results, it is reasonable to determine that the eigenmode of figure 4(a) is TEM 40. The spectral line figure 4(b) is confused with figure 4(a) when only compared with equipotential contours. The peak positions of electric equipotential are similar to each other. Also, the shapes of these spectra are similar to each other. However, looking closely at their location and shape, there are clear differences. The extreme position of equipotential (b) is located slightly upper than that of that of (a). And the peak of the equipotential line is stronger in (b) compared to (a). Comparing the distribution of the electric field between figures (a) and (b), there are clear difference. It is certain that the electric field (b) is more widely distributed than that of (a) in y-direction. The peak of the electric potential is established by another mode which do not the same as that of x-direction. It is certain that the eigenmode is dominated by this characteristic. Therefore, it is reasonable to determine the eigenmode of figure 4(b) to be TEM 31. The equipotential spectra shown in figure 4(c) reveal similar appearances as that of (d). However, careful observation of the spectra (c) and (d) shows that the electric field component of (d) in the y-axis direction is distributed slightly upward than in the case of (c). This means that in the case of (d), another eigenmode component exists in the ydirection as like (b). Based on this discussion, it is reasonable to determine the eigenmodes of (c) and (d) as TEM 20 and TEM 21, respectively. The most confusing factor in determining eigenmodes is the y-component. This component is affected by the conductor plane placed between the dielectrics. The electric field is incident only perpendicularly around the conductor plane. This property imposes constraints on the eigenmodes formed in the waveguide. This effect of the conductor creates similar but different modes when generating eigenmodes. The results reflecting this property are revealed through eigenmodes such as (c) and (d). Here, Electric fields clearly appear on the left and right sides of the waveguide, but the presence of potentials is imprecise. This is presumed to be due to the presence or absence of the y-component. A detailed analysis of this is deferred to the next study. Figure 4(e) can be identified in the same context as discussed above. A potential peak is formed at the edge of the conductor plane. And the strength of the electric field is strongly formed there. Potential is strongly formed on the left and right sides of the waveguide, but the electric field does not take such a strong form. However, when considering the spatial distribution of potentials as a criterion, this spectrum can be regarded as TEM 20.

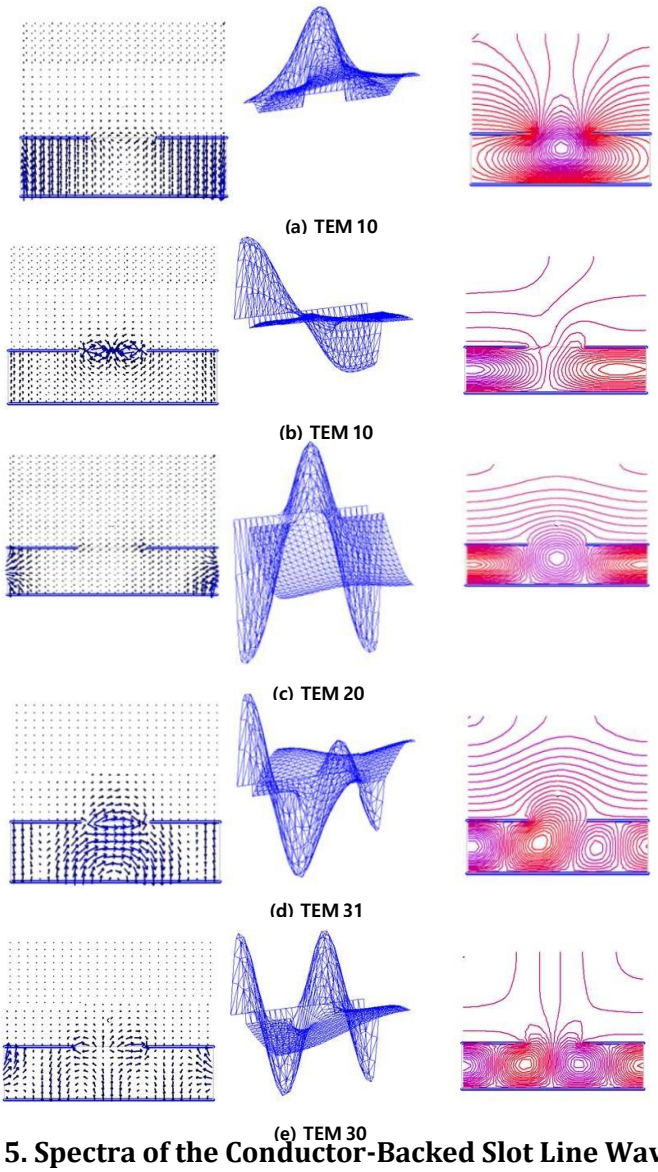


Figure 5. Spectra of the Conductor-Backed Slot Line Waveguide

Figure 5 is schematic representation of the spectra for a CBSLW. Two conductor plates over the dielectric and another backed conductor have great impact on determining the eigenmodes of electromagnetic waves. As mentioned earlier, they impose constraints on electromagnetic waves when forming eigenmodes. The electric field incident the conductor perpendicularly. The electric field cannot penetrate the conductor. The electric field leak through the slot. Figure 5 shows the eigenmodes formed by an electric field confined to the dielectric and escaping through the slot. The eigenmodes reveal mostly symmetric or antisymmetric forms. Figure 5(a) shows a symmetrical spectrum of a typical CBSLW with an eigenmode of TEM 10. Figure 5(b) shows the anti-symmetrical spectrum of a typical CBSLW with an eigenmode of TEM 10. If the resolution of the electric field spectrum is low, it can be supplemented through the spatial distribution of electrical equipotential lines. The electric field distributed at the edge of the conductor in the entrance region of the slot shows TEM 10 while exhibiting antisymmetry. The intensity of the electric field in this region is greater than in other regions, but it is difficult to

confirm its existence on the equipotential line. In the overall context, further studies are needed to determine the relationship between the eigenmodes of this region and the electric field distributed. Figure 5(c) shows the spectrum where the electric field and potential follow a symmetrical spatial distribution. Equipotential lines showing relatively strong intensity are distributed in the left and right sides region of the waveguide. The peak of the electric equipotential is placed at the central region of dielectric layer of the waveguide. In this region, the electric field shows a weak intensity, so it does not play a leading role in determining the eigenmode. The spatial distribution of equipotential lines alone is sufficient to determine the eigenmodes. In other words, when determining the eigenmode, the electric field and potential complement each other to make a correct decision. Through this relationship, the eigenmode in figure 5(c) is determined to be TEM 20 based on the equipotential. Figure 5(d) and (e) are the spectra representing the eigenmodes TEM 31 and TEM 30, respectively. The spectrum of figure 5(d) shows the spatial distribution of the symmetrical electric field in the waveguide. However, equipotential lines are distributed asymmetrically unlike electric fields. The upper part of the second peak of the equipotential line is located slightly to the right. Two reasons are presumed for this. The first is a small potential component locating in the y-direction. It is presumed that this component is added to the base potential to create an overall asymmetric structure. The second reason is presumed that the top conductor of the dielectric suppresses the spatial distribution of potential. It is presumed that these two causes combine to make the spatial distribution of electrical potential slightly asymmetrical. Therefore, the eigenmodes in figure 5(d) is determined to be TEM 31 by combining the electric field and the electric equipotential. In the spectrum of figure 5(e), the spatial distribution of electric field and equipotential reveal symmetrical and well balancing in the waveguide. Therefore, the eigenmode of the spectrum in figure 5(e) are determined to be TEM 30.

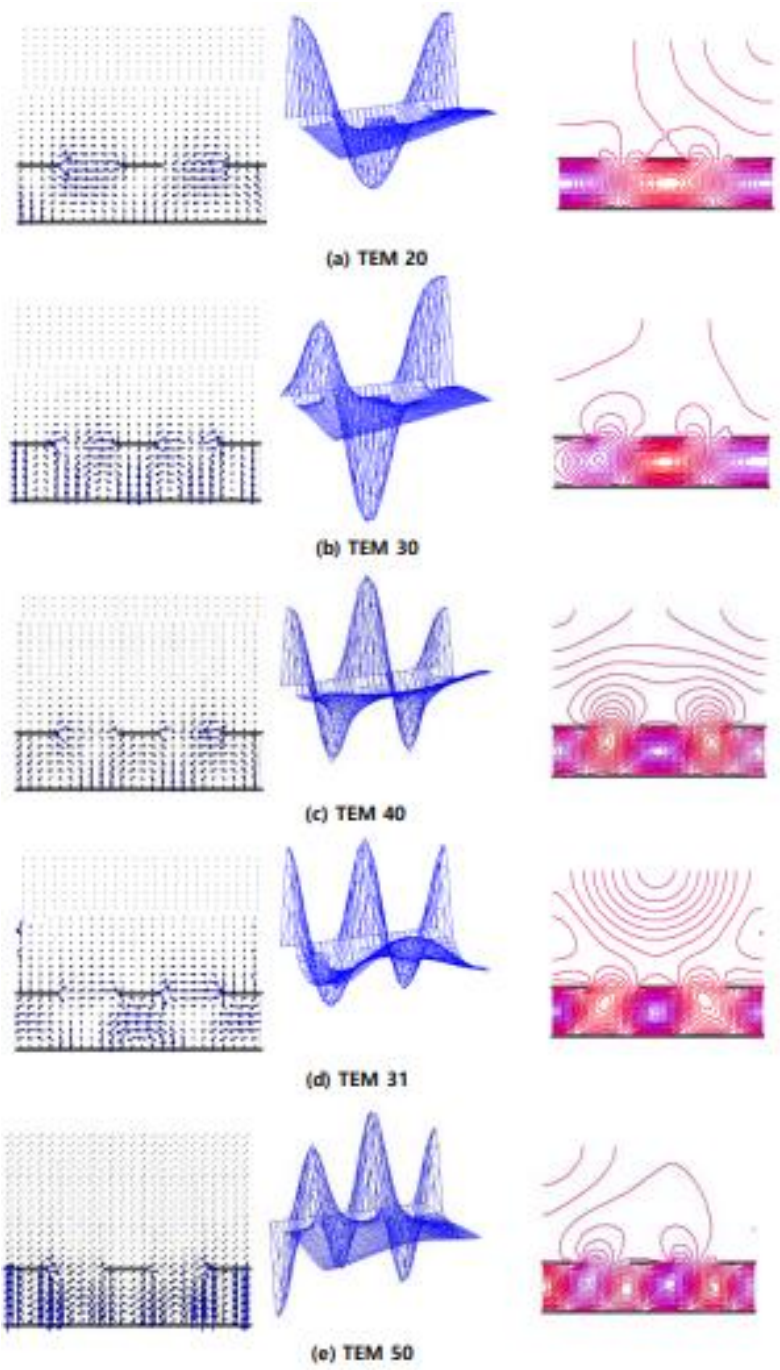


Figure 6. Spectra of the Conductor Backed Coplanar Waveguide

Figure 6 is schematic representation for the spectra of CBCPW. All spectra form prominent eigenmodes in the waveguide without any significant distortion. This is due to the conductor plates placed on the top of the dielectric and another metal plate on the back surface. These conductor plates not only confine electromagnetic waves between them, but also contribute to the construction of unique eigenmodes. The determination of the eigenmodes corresponding to these spectra is not a problem and is determined easily using the distribution of the electric

field and the location of the equipotential peaks. The eigenmodes for each spectrum are determined based on those previously discussed. The eigenmode thus determined for each spectrum is displayed under each one. What is unique about the CBCP waveguide is that as eigenmodes number increases, the corresponding spectrum becomes more complex. However, since the shape of the spectrum is distinct, it does not make any problems in determining eigenmode.

CONCLUSION

In this study, the eigen mods of the CPW, CBSL and CBCP waveguides have been calculated by FEM. In this calculation, the dimension of the equation of the eigen matrix were so large that Krylov-Schur iteration method has been applied. The eigenmodes have been represented with the electric field, 3D electric potential and electric equipotential. The electric field and electric potential have been compensated each other to identify the eigenmodes of the waveguides more clearly. Using these, the analysis of the low-resolution spectrum was performed with high reliability. In particular, the use of 3D and equipotential contours with the electric field made it possible to interpret the spectrum of overlapping peaks that had not been identified in previous studies. From these results, it would be expected that the analysis and understanding of the physical property, in which eigenmode is complicated by the influence of the conducting plate, will be more improved by utilizing complementary elements.

References

[1]. Yeong Min Kim, A Study on the Eigenmodes Constructed in the Conductor Backed Coplanar Waveguide. Transactions on Engineering and Computing Sciences, Jun 2023,11(3).108-121.

[2]. Wen, C. P., *Coplanar Waveguide, a Surface Strip Transmission Line Suitable for Nonreciprocal Gyromagnetic Device Applications*, IEEE Trans. on Microwave Theory and Techniques, 1969, Vol. 17, No.12, pp.1087-1090.

[3]. N. RAINEE SIMONS, Coplanar Waveguide Circuits, Components, and Systems, A JOHN WILEY & SONS, INC., PUBLICATION, 2001, pp. 87-111.

[4]. John Coonrod, Brian Rautio, Comparing Microstrip and CPW Performance, MICROWAVE JOURNAL, July 2012 Vol. 55, No. 7, pp.74-82.

[5]. C. J. Reddy, Manohar D. Deshpande, C. R. Cockrell, and Fred B. Beck, Finite Element Method for Eigenvalue Problems in Electromagnetics, NASA Technical Paper, Dec. 1994, 3485.

[6]. Yeong Min Kim, Se Jung Oh, The Eigen-Properties Constructed in the HAPCF, HSST, November 2018, Vol.8, No.11.

[7]. G. W. Stewart, "A Krylov Schur Algorithm for Large Eigenproblems". (2002) SIAM J. Matrix Anal. & Appl. Vol. 23, No. 3, pp. 601-614.